Hybrid Nanofluids for Solar Thermal Process Heating Applications

Satish Upadhyay[1, 2, #], Laltu Chandra[1, 3], Jahar Sarkar[1]
[1]Department of Mechanical Engineering, IIT (BHU) Varanasi (India).
[2] uGDX School of Technology, ATLAS SkillTech University Mumbai, (India).
[3]Department of Sustainable Energy Engineering, IIT Kanpur, (India).
[#]Correspondence: satishupadhyay.rs.mec18@itbhu.ac.in

Abstract

Experiments with turbulent flow of hybrid nano-oils are reported to mitigate the dearth of experimental data for assessing the developed generalized Nusselt number correlation, deduced using separation approach. A controlled, Joule-type, uniform heating condition is adopted for simplicity. The significant findings are (a) the Nusselt number enhanced with the addition of nano-particles, (b) the addition of nanoparticles increases the pressure drop and (c) the assessment of Figure of Merit confirms that the use of hybrid nano-oil is beneficial compared to pure oil, and (d) the generalized Nusselt number correlations are applicable for hybrid nano-oils within the reported uncertainty of $\pm$ 15%. Therefore, the experiment is a step towards utilization of hybrid nano-oils as heat transfer fluid for heat transfer applications.

Keywords: Experiment, hybrid nano-oil, Nusselt number, turbulent flow

Introduction

Solar energy is freely available and is widely used for process heating and cooling applications. In Industries, many applications lie in the medium temperature range of 353 – 573 K, discussed by Pranesh et al. (2019). Concentrating Solar Thermal systems can fulfill this demand; in this Parabolic Trough collector is the most mature technology, which is expected to save to save fossil fuel, enhance the system efficiency, and mitigate the emission of greenhouse gases. Such systems require heat transfer fluids (HTFs) to transport the heat generated significantly by reflected solar irradiance to the applications for heating or cooling. (Vignarooban et al., 2015). A parabolic trough collector (PTC) absorber is exposed to peripherally non-uniform concentrated heat flux, and a heat transfer fluid is utilized to recover the generated heat via forced convection. Interestingly, the use of a secondary reflector is one method to reduce the non-uniformity. Tang et al. (2021) discussed how to achieve uniform heat flux distribution by optimizing the design of the secondary reflector of PTC. Various research focused on HTF-like nanofluid and hybrid nanofluid and reported an enhancement in efficiency and Nusselt number. Various Nusselt number correlation, specific to nanofluid, and also the generalized Nusselt number correlation deduced by separation approach is discussed in detailed by Upadhyay et al. (2021, 2022). Krishna et al. (2018) thoroughly reviewed experimental and numerical work utilizing nanofluid in PTC. Literature suggested use of hybrid nanofluid over nanofluid (Tiwari et al., 2021). Thus hybrid nanofluid is selected for experimental work.

The literature review revealed the need for heat transfer experiments with hybrid nano-oil. Therefore, experiments are performed with Therminol VP1 (TVP1) and 1% (V/V) Al_2O_3-CuO-TVP1 hybrid nano-oil subjected to uniform heat flux conditions assuming PTC absorber consisting of secondary reflector to homogenize the solar radiation to get uniform heat flux. The objective is to find experimental heat transfer enhancement with hybrid nano-oil for turbulent flow and assess the generalized Nusselt number correlation developed for an oil-based hybrid nanofluid experimentally. The paper presents the preparation and stability of the oil-based hybrid nanofluid, the developed experimental setup, the heat transfer coefficient, and Nusselt number. To the best of the authors' knowledge, no such detailed experiments with hybrid nano-oil are reported thus far. The details of the experiment setup, the adopted procedure, and the findings are presented subsequently.

1. Experimental setup and procedure

The schematic of the forced convection experimental setup is shown in Figure 1. It comprises a heat transfer fluid tank (HTF tank), pump, bypass valve, flow meter, test section (heated and unheated section), U-tube manometer,

10.18086/swc.2023.03.12 Available at http://proceedings.ises.org

power supply, and chiller. HTF tank stores sufficient fluid, which is supplied as soon as the pump is turned on. Initially, the HTF is heated by an immersion heater placed inside the HTF tank up to the desired inlet fluid temperature (T_{in}) and a chiller is used to maintain the steady operating condition. A one-horsepower pump is used to circulate the HTF through the test section, including the chiller. A bypass valve is installed to control HTF's flow and attain the desired flow rate during the experiment. A turbine-type flow meter is installed to record the flow rate in liters per minute (LPM). The test section comprises a 4 m long, straight, horizontal copper tube depicting a PTC absorber with an external heating element. The test section (copper tube) is divided into two parts, viz. unheated and heated length of 2 m, the outer diameter of the tube is 0.025 m, and the inner diameter of the tube is 0.023 m. Thus, a sufficient length-to-diameter ratio of ~86 is provided to attain the heated copper tube's hydraulically fully developed inflow condition.

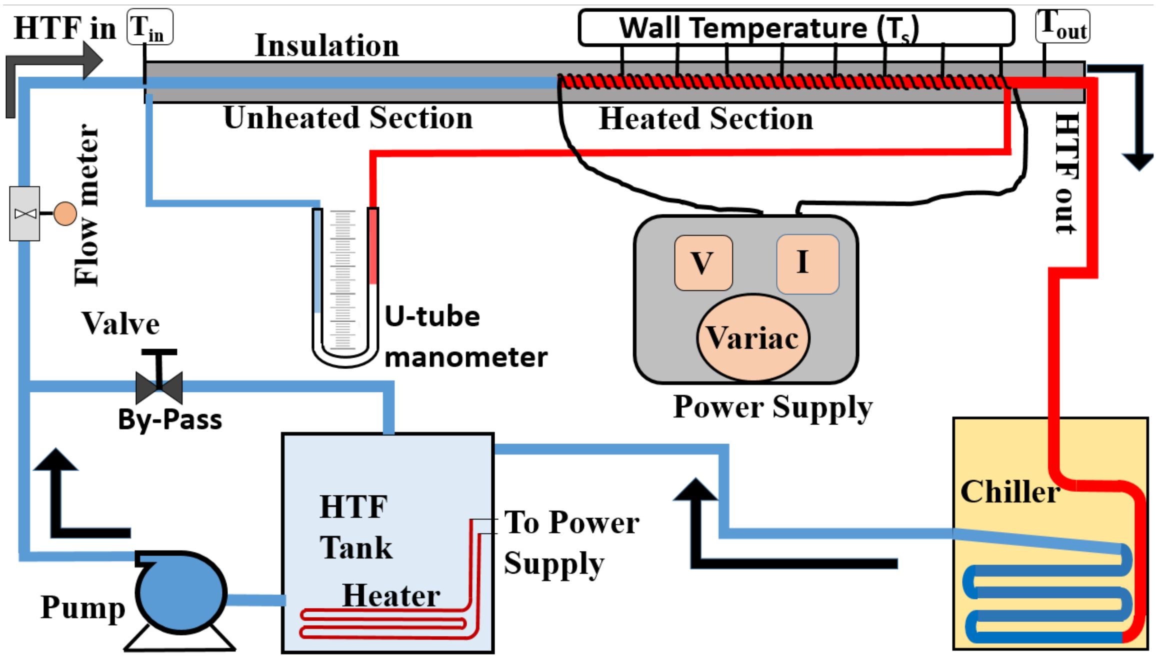

Figure 1. Schematic of the installed experiment setup for the heat transfer with therminol and hybrid nano-oil.

Figure 1 illustrates that K-type thermocouples and a data acquisition (DAQ) system are installed to record the inlet, outlet, and outer wall temperatures. A U-tube manometer is installed to measure the pressure drop across the straight tube using the height of the mercury column. The test section is externally insulated, with sufficient thickness, to mitigate heat losses. It is worth mentioning that the inlet and outlet of the test section are provided with a wire mesh to promote mixing and redistribution of HTF temperature. Therefore, as far as possible, the measured temperatures are interpreted as the bulk mean. The measured parameters, the corresponding instruments, their range, and accuracy details are provided in Table 1.

Table 1. The measured parameters, instruments, and their operating range/accuracy

Parameters	**Instruments**	**Range**	**Accuracy**
Flow rate	Turbine-type flowmeter	10 to 50 LPM	±0.1 LPM
Temperature	K-type thermocouple	20 to 300 ºC	±0.1 ºC
Wattmeter	Wattmeter, Specification: 250 V, 50 Hz, Maximum 10 A	Less than 2.2 KW	±0.25%

A photograph of the installed experimental facility is shown in Figure 2a. The externally insulated, long, straight test section (copper tube), including thermocouples, is wrapped with nichrome wire as a heating element (see Figure 2b). Silicon rubber is provided between the unheated and heated part of the test section to mitigate the heat transfer, as far as possible, during the experiment. K-type thermocouples are installed on the outer wall of the copper tube using a groove of 0.5 and a high-temperature epoxy. Due care is taken to isolate the thermocouple sensor from the heating element by utilizing insulation around the same. The thermocouples are uniformly spaced (25 cm) along the axial direction on the heated section, and some probes are placed along the circumferential direction to record azimuthal variation, if any, for the applied boundary conditions. Several efforts were made to perform the experiments for uniform and non-uniform heat flux distributions along the azimuthal direction. However, achieving a non-uniform heat flux distribution depicting discrete heating conditions was not possible using the installed nichrome wire-wrapped copper tube. The authors finally concluded that the same can be attained, possibly by using an external radiation source, and is of future interest. However, the current experiment provided helpful data for the assessment of the generalized Nusselt number correlation for hybrid nano-oil. The installed, multiple K-type thermocouples at the inlet and outlet near the wire mesh are shown in Figure 2c.

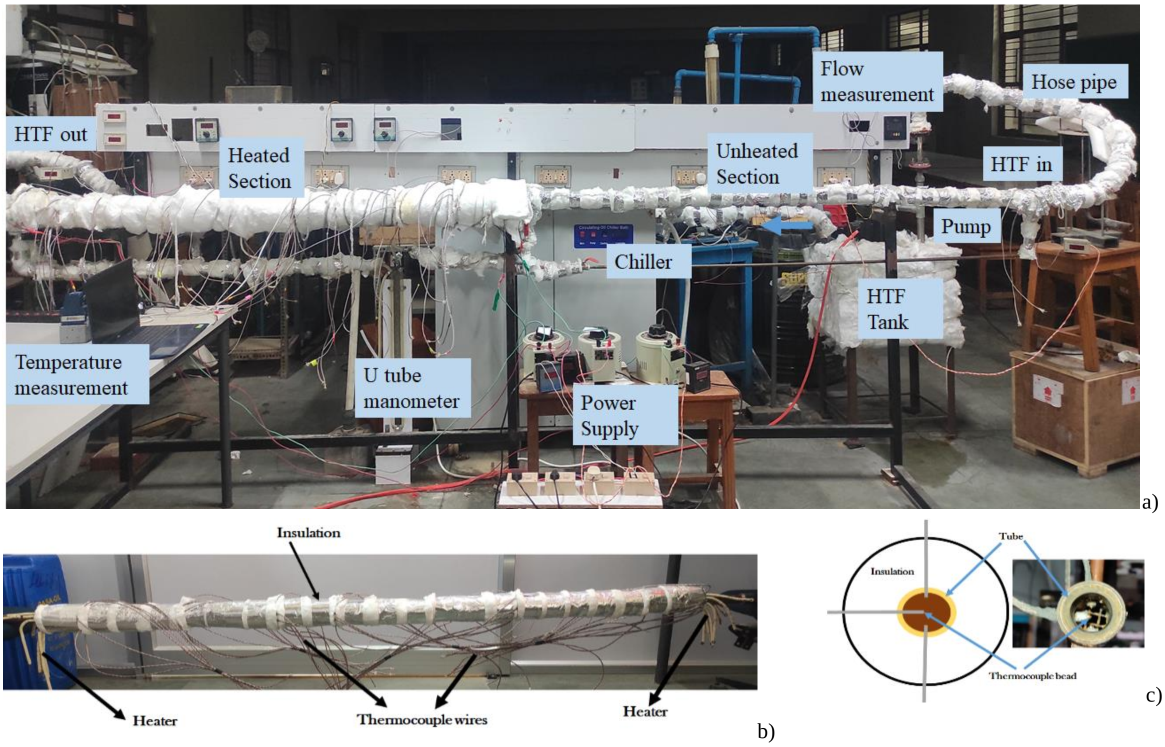

Figure 2. Photograph of a) the installed experimental setup for heat transfer with oil and hybrid nano-oil, b) the installed, externally insulated heating section with thermocouples, and c) the installed thermocouples at the inlet and outlet to measure fluid temperature.

The following step-wise approach is adopted for performing the experiments:

Step 1: The HTF is heated to the desired inlet temperature, and the flow rate is steadily increased to attain the desired flow rate or the corresponding Reynolds number in the range of 7000 - 19000. Subsequently, the flow is allowed to stabilize for some time.

Step 2: The power supply is turned on, and the same is regulated using a variac. This is measured using a wattmeter, and the same is verified using the attached voltmeter and ammeter. This allows external heating of the 2 m long test section.

Step 3: The system is allowed to operate and stabilize. Once the steady state is attained, the flow rate, inlet, outlet, and wall temperatures are recorded.

Following the adopted procedure, the HTF is heated to attain the inlet temperature of 353 K. The flow rate of HTF is maintained at a value between 10 – 26 LPM with an increment of 2 LPM. The first set of experiments is performed with TVP1 oil, and the second set of experiments is performed for 1% (V/V) Al_2O_3-CuO TVP1 hybrid nano-oil. The input power to the 2 m long, straight copper tube is maintained at 3.2 kW for all the experiments. Achieving a higher power was challenging because of safety-related issues in the laboratory. Several parameters are noted for the experiment after attaining a steady state. This was inferred from the test section's measured fluid and solid temperatures. The thermophysical properties of pure oil and hybrid nano-oil are adopted from various literature shown in Table 2. Thus, after calculating the thermophysical properties and using the appropriate equations presented later in the data deduction, the Nusselt number and friction factor are calculated and compared with the standard correlation discussed in section 3.

Table 2. Thermophysical property of Therminol VP1 and hybrid nano-oil.

Material/oil/ nano-oil	Equations/correlations
TVP1 (Mwesigye et al. 2017, Klein, 2017)	$\rho = 1.4386 \times 10^{-3} - 1.8711T + 2.737 \times 10^{-3}T^2 - 2.3793 \times 10^{-6}T^3$ (kg m^{-3}) $c_P = 2.125 \times 10^3 - 11.017T + 0.049862 \times T^2 - 7.7663 \times 10^{-5}T^3 + 4.392 \times 10^{-8}T^4$ (J kg^{-1}K^{-1}) $\lambda = 0.14644 - 2.0353 \times 10^{-5}T - 1.9367 \times 10^{-7}T^2 + 1.0614 \times 10^{-11}T^3$ (W m^{-1}K^{-1}) $\mu = 0.023165 - 0.1476 \times 10^{-3}T + 3.617 \times 10^{-7}T^2 - 3.9844 \times 10^{-10}T^3 + 1.6543 \times 10^{-13}T^4$ Pa.s
Hybrid nanofluid (Upadhyay et al. 2021, Mwesigye et al. 2017, Pak et al. 2013, Xuan et al. 2000)	$\rho_{hnf} = (1-\phi)\rho_{bf} + \phi_1\rho_{np1} + \phi_2\rho_{np2}$ (kg m^{-3}), where $\phi = \phi_1 + \phi_2$ $C_{phnf} = \frac{(1-\phi)\rho_{bf}C_{pbf} + \phi_1\rho_{np1}C_{pnp1} + \phi_2\rho_{np2}C_{pnp2}}{\rho_{hnf}}$ (J kg^{-1}K^{-1}) $\lambda_{nf} = \left[(3\phi-1)k_{np} + (2-3\phi)k_{bf} + \sqrt{\Delta}\right]$ (W m^{-1}K^{-1}) where $\Delta = \left[(3\phi-1)k_{np} + (2-3\phi)k_{bf}\right]^2 + 8k_{np}k_{bf}$ (W^2 m^{-2}K^{-2}) $\lambda_{hnf} = \frac{k_{nf1}\phi_1 + k_{nf2}\phi_2}{\phi}$ (W m^{-1}K^{-1}) $\mu_{hnf} = \mu_{bf}(123\phi^2 + 7.3\phi + 1)$ (Pa s)

2.1. Hybrid nano-oil preparation: Al_2O_3-CuO TVP1

Hybrid nano-oil is prepared by mixing an appropriate fraction of Al_2O_3 and CuO nanoparticles in TVP1. In general, 1g of hybrid nanoparticles comprises 0.8g of Al_2O_3 and 0.2 g of CuO nanoparticles. Thus, to prepare 1% (V/V) of hybrid nanofluid, 395.4 g of Al_2O_3 and 98.84 g of CuO nanoparticles are dispersed in 11 L of TVP1 oil. The high-precision electronic weighing machine (model: SWIL 220, India) is used to measure the weight of nanoparticles and surfactants with a resolution of 0.1 mg. The measured quantity of nanoparticles is mixed in TVP1 with a magnetic stirrer (Tarsons Digital Spinot) for more than 2 hours. Subsequently, for proper dispersion of the hybrid nanoparticles, Sodium Dodecyl Sulfate (SDS) is used Gimeno-Furio at al. (2017). After stirring, the solution is sonicated in the ultrasonicator (Labman Scientific Instruments, India) for more than 2 hours. The steps for hybrid nano-oil preparation are shown in Figure 3. The stability of the prepared hybrid nano-oil is inspected by two methods, viz. a) visual inspection and b) pH Value. The concept of isoelectric point (IEP) is used to test the stability of a hybrid nanofluid by its pH value. The stability of a hybrid nanofluid can be ensured if its pH value is far from the isoelectric point of nanoparticles (Kumar et al., 2019). This is attributed to a large repulsive force between the suspended nanoparticles in the base fluid. For example, the isoelectric point of Alumina nanoparticles is 9.1 (Singh et al., 2005), and that of copper oxide nanoparticles is 10 (Sousa et al., 2013). The pH value is measured by a pH meter (model: CL 54+Toshcon Industries, India). The pH meter is calibrated before measurement, and the measurement is repeated three times. The stability of the hybrid nano-oil is discussed in section 3.1

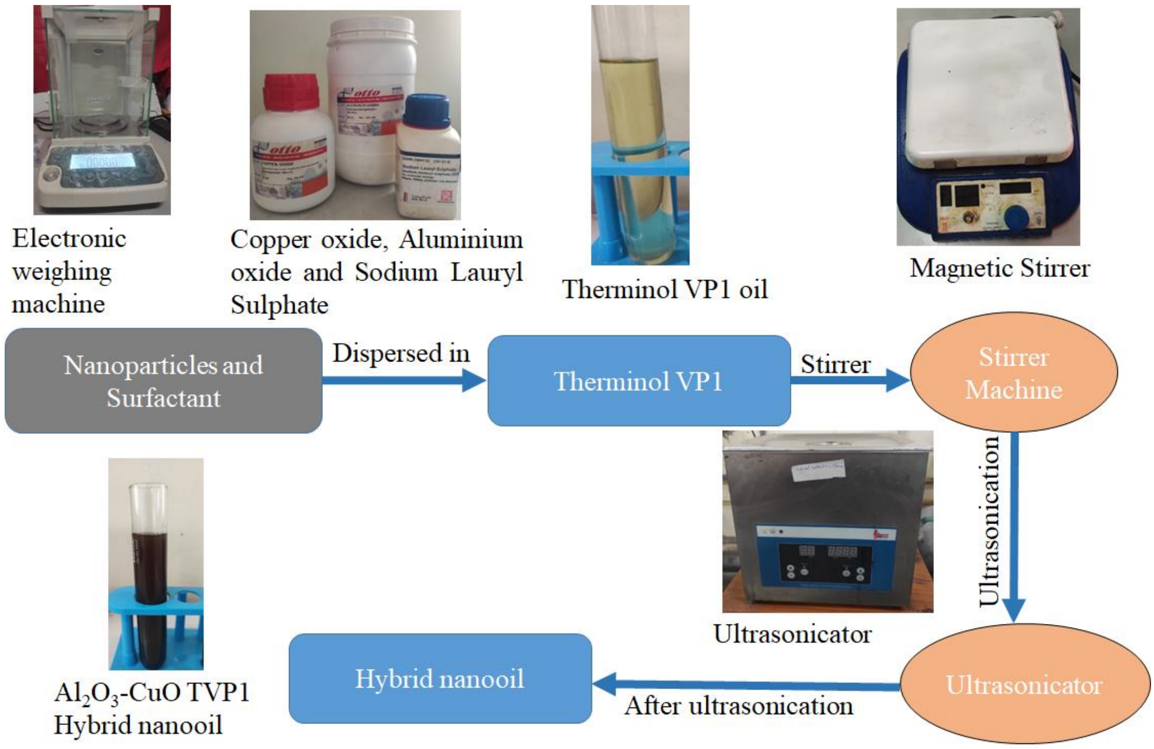

Figure 3. Equipment used and steps for the preparation of hybrid nano-oil.

2.2. Data Deduction

To calculate the Nusselt number and friction factor, the following equations are used:

Rate of electrical heat input: $\dot{Q}_{electrical} = VI$ (eq. 1)

Rate of heat removal by HTF: $\dot{Q}_{absorbed} = \dot{m}c_p(T_{out} - T_{in})$ (eq. 2)

The recorded heat loss rate $\left(\dot{Q}_{electrical} - \dot{Q}_{absorbed}\right)$ is less than 3% of the rate of electrical power input. The surface-area averaged convective heat transfer coefficient is obtained by Newton's law of cooling, as follows:

$$\bar{h} = \frac{\dot{Q}_{absorbed}}{A(T_s - T_b)} \quad \text{(eq. 3)}$$

where $T_s = \frac{\sum_{i=1}^{8} T_{si}}{8}$ K, $T_b = 0.5(T_{in} + T_{out}), A = \pi(D_{in}L)$, T_{in} is the inlet temperature of the fluid, T_{out} is the outlet fluid temperature of the fluid, T_s is the average wall temperature, T_b is the mean bulk fluid temperature, A is the inner surface area of the tube, L is the heated length of the tube, and D_{in} is the inner diameter of the tube.

Experiment-based average Nusselt number and friction factor are calculated as follows:

$$\overline{Nu} = \frac{\bar{h}D_{in}}{k} \quad \text{(eq. 4)}$$

$$f = \frac{\Delta P}{\frac{L}{D_{in}}\left(\frac{\rho V^2}{2}\right)} \quad \text{(eq. 5)}$$

The experimentally calculated Nusselt number is compared with the generalized Nusselt number correlation for hybrid nanofluid and is discussed in results and discussion. The deduced generalized Nusselt number correlation and Figure of Merit (FoM) taken from Upadhyay et al. (2021, 2022) are as follows:

$$Nu_{gen} = \underbrace{1.01\alpha_r^{0.08879}\phi^{0.0542}n^{-0.1482}}_{\eta} \underbrace{\left\{\frac{\frac{f}{8}(Re-1000)Pr}{1+12.7\sqrt{\frac{f}{8}}\left(Pr^{\frac{2}{3}}-1\right)}\right\}}_{\textit{Gnielinski correlation},\ Nu_{bf}} \quad \text{(eq. 6)}$$

$$FoM = \frac{Nu}{CP}, \text{ where } CP = \frac{\Delta P}{0.5\rho V^2}, \quad \text{(eq.7)}$$

2.3. Uncertainty Analysis

The various parameters like dimension, flow rate, temperature, and power input are measured by vernier caliper, turbine flowmeter, k-type thermocouple, and wattmeter, respectively. The uncertainty calculation for the dependent parameters such as Reynolds number, Prandtl number, heat transfer rate, convective heat transfer coefficient, Nusselt number, friction factor, coefficient of pressure, and Figure of Merit are calculated using the following eq. (8) (McClintock et al., 1953).

$$U_z = \left[\left(\frac{\partial Z}{\partial X_1} i_1\right)^2 + \left(\frac{\partial Z}{\partial X_2} i_2\right)^2 + \left(\frac{\partial Z}{\partial X_3} i_3\right)^2 + \dots\dots\dots + \left(\frac{\partial Z}{\partial X_n} i_n\right)^2\right]^{\frac{1}{2}} \qquad \text{(eq. 8)}$$

Where, $i_1, i_2, i_3, \dots\dots\dots, i_n$ are the uncertainties of the independent variables, and Z is a function of the independent variables X_1, X_2, X_3,…, X_n.

Table 3. Uncertainty estimation for different experiment-based parameters

Parameters	**Uncertainty (%)**
Heat transfer rate	±2.8331
Reynolds number	±2.8372
Prandtl number	±3.4641
Convective heat transfer coefficient	±2.8402
Nusselt number	±3.474996
Pressure drop	±2.2362
Coefficient of pressure (*CP*)	±3.0099
Figure of merit (FoM)	±4.6581

2.4. Validation

The experiment-based average Nusselt number for pure TVP1 are compared with the Gnielinski correlation (see figure 4). The measured values are found well within ±10%. With the increasing Reynolds number from 7000 to 19000 the turbulent intensity increases. Consequently, the Nusselt number increases with the increasing Reynolds number, as expected.

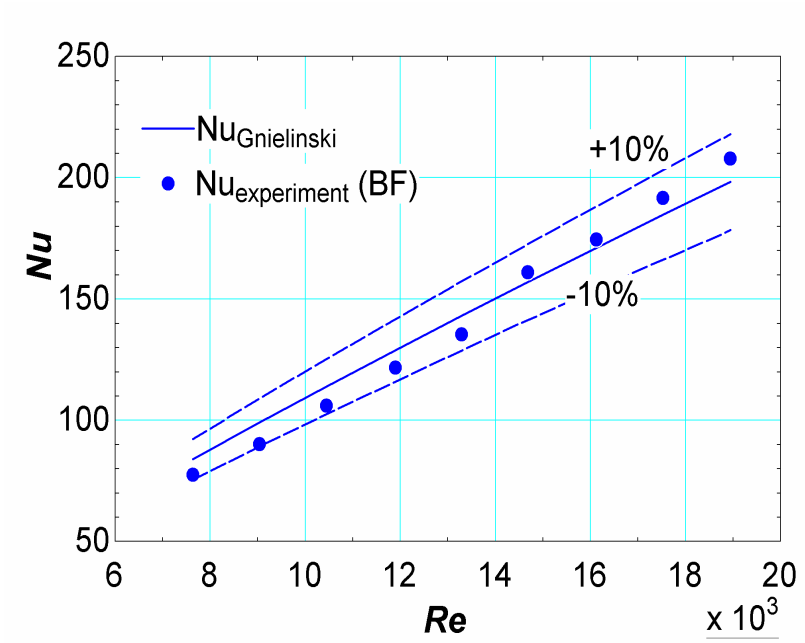

Figure 4. Comparison between the experiment-based Nusselt number and Friction factor with Gnielinski correlation

2. Results and discussion

3.1. Hybrid Nanofluid: Stability

Figure 5 displays the samples of pure TVP1 and Al_2O_3-CuO-TVP1 hybrid nano-oil. The stability of the hybrid nano-oil is assessed through visual inspection. Figure 5b to 5f presents the photograph of hybrid nano-oil that is captured at different time intervals immediately after preparation (day 0) and after one, two, three, and four days of preparation. In particular, until day 2 (Figure 5d), there is no practical visual evidence of nanoparticle sedimentation, indicating that the hybrid nano-oil remains stable during this period. However, after day 2, minor sedimentation becomes evident (see Figure 5d), suggesting some settling of nanoparticles in the fluid. Apart from visual inspection, the stability of the prepared hybrid nano-oil is also inspected by the concept of an isoelectric point (IEP). The IEP of Al_2O_3 is 9.1, and for CuO, it is 10, which are both significantly far away from the measured pH value of 5.1 for the hybrid nano-oil. This difference supports the stability of hybrid nano-oil. Furthermore, the experiments are conducted continuously, meaning that any sedimentation process occurring beyond day 2 is unlikely to affect the experimental outcome significantly. Therefore, the stability of the hybrid nano-oil throughout the experiment is reasonably assured, and the results obtained from the tests remain reliable.

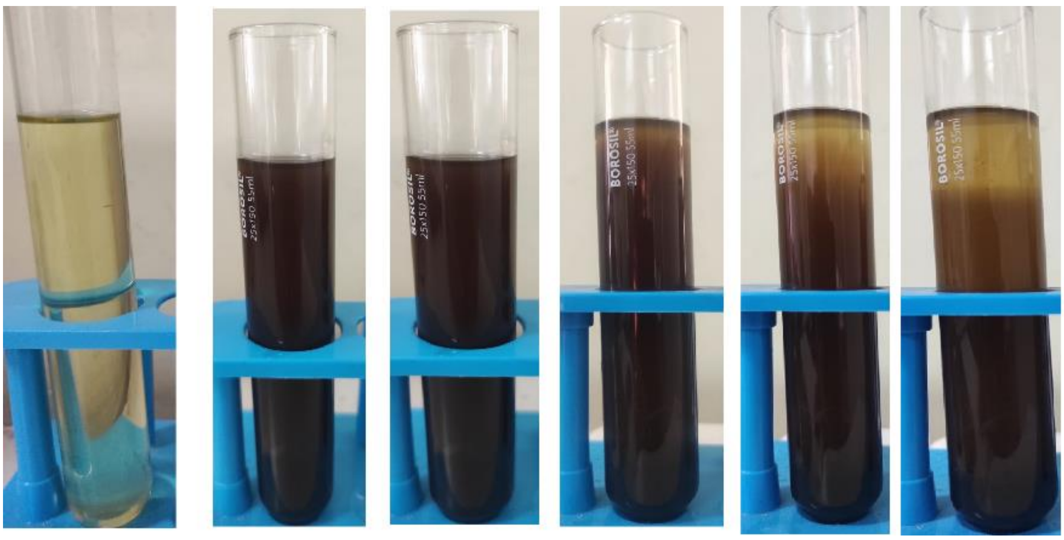

a) b) c) d) e) f)

Figure 5. Photograph of a) TVP1, (b)-(f) 1% (V/V) Al_2O_3-CuO-TVP1 hybrid nano-oil after (b) day 0, (c) day 1, (d) day 2, (e) day 3 and (f) day 4.

3.2. Convective Heat Transfer Coefficient and Nusselt Number: Oil and Hybrid Nano-oil.

The experiments are conducted using a carefully prepared 1% (V/V) Al_2O_3-CuO-TVP1 hybrid nano-oil, with flow rates ranging from 10 to 26 LPM, increasing in increments of 2 LPM. The objective is to compare the heat transfer characteristics of pure TVP1 oil and the Al2O3-CuO-TVP1 hybrid nano-oil. Figure 6a illustrates the comparison of experiment-based surface-area averaged heat transfer coefficient for both fluids, while Figure 6b presents a similar comparison for the experimental calculated Nusselt number.

The results demonstrate notable improvements in both the surface-area averaged heat transfer coefficient and Nusselt number when using the hybrid nano-oil compared to pure oil. Specifically, the Nusselt number for the hybrid nano-oil increases by approximately 15% compared to pure oil. This enhancement in heat transfer performance indicates that the use of hybrid nano-oil can significantly improve the thermal efficiency of the system. Consequently, the surface area required for a Parabolic Trough Collector (PTC) absorber, which is the heart of PTC-based concentrated solar thermal system, can be reduced by about 15% for a given temperature difference and input power compared to pure oil. This reduction in surface area is a substantial benefit, as it can lead to cost savings and increased overall system performance for concentrated solar thermal systems. Thus, the use of hybrid nano-oil seems favorable for concentrated solar thermal systems. However, while the heat transfer benefits of the hybrid nano-oil are promising, one question remains: is the pressure drop favorable for the turbulent flow of the hybrid nano-oil? The pressure drop is a critical factor, and it is essential to consider the impact of pressure drop in the turbulent flow of the hybrid nano-oil. This is discussed subsequently.

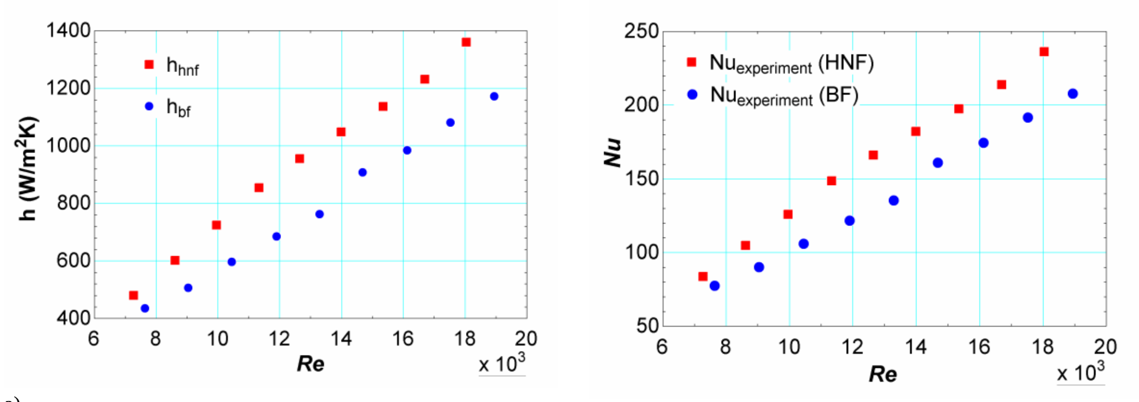

a) b)

Figure 6. a) Convective heat transfer coefficient and b) Nusselt number for TVP1 and Al_2O_3-CuO-TVP1 hybrid nano-oil.

3.3. Pressure drop: Oil and Hybrid Nano-oil

Figure 7 comprehensively compares the measured pressure drops between pure TVP1 oil and Al_2O_3-CuO-TVP1 hybrid nano-oil. The observations are twofold: (a) the pressure drop increases with the volume flow rate for both pure oil and the hybrid nano-oil, and (b) the turbulent flow of the Al_2O_3-CuO-TVP1 hybrid nano-oil experiences, on average, approximately 12% higher pressure drop compared to TVP1 across the considered volume flow rates. This suggests that using the hybrid nano-oil in the PTC absorber will necessitate a higher pumping power than the pure TVP1, indicating a disadvantage associated with using the hybrid nano-oil in terms of increased energy consumption for fluid circulation.

Despite the drawback of higher pumping power, it is vital to assess if there are any relative benefits in terms of heat transfer performance with the hybrid nano-oil compared to the pressure drop. To address this question, the proposed figure of merit (FoM = *Nu*/*CP*), where *Nu* represents the averaged Nusselt number and *CP* is the coefficient of the pressure of the fluid, is considered. These parameters are discussed subsequently for both pure oil and the hybrid nano-oil.

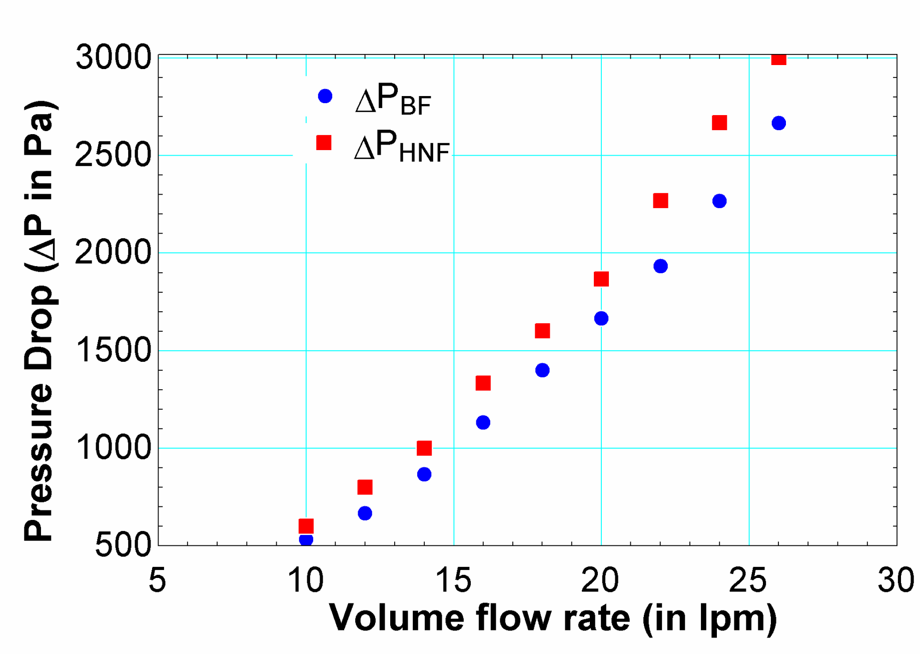

Figure 7. Pressure drop versus volume flow rate for TVP1 and Al_2O_3-CuO-TVP1 hybrid nano-oil.

3.4. Figure of Merit: Oil and Hybrid Nano-oil

A comprehensive analysis of the figure of merit (FoM) has been conducted to evaluate the performance of pure TVP1 oil and the Al_2O_3-CuO-TVP1 hybrid nano-oil for concentrated solar thermal systems. A non-dimensional parameter, viz. ratio of the Nusselt number to the coefficient of pressure ratio (*Nu/CP*), represented by the FoM, is plotted in Figure 8. This analysis aims to evaluate the relative benefits of using the hybrid nano-oil compared to pure oil in concentrated solar thermal systems. The findings from Figure 8 indicate that the experiment-based FoM for the hybrid nano-oil is approximately 5-6% higher than that of pure oil. This significant improvement in the FoM for the hybrid nano-oil implies, despite experiencing a higher pressure drop, that the hybrid nano-oil exhibits a significantly superior Nusselt number compared to the penalty incurred from the increased friction factor. Based on the comprehensive experimental investigation and the analysis of the FoM, it is concluded that the Al_2O_3-CuO-TVP1 hybrid nano-oil can be recommended as the preferred choice for PTC-absorber in comparison to pure TVP1 oil for PTC-based concentrated solar thermal systems.

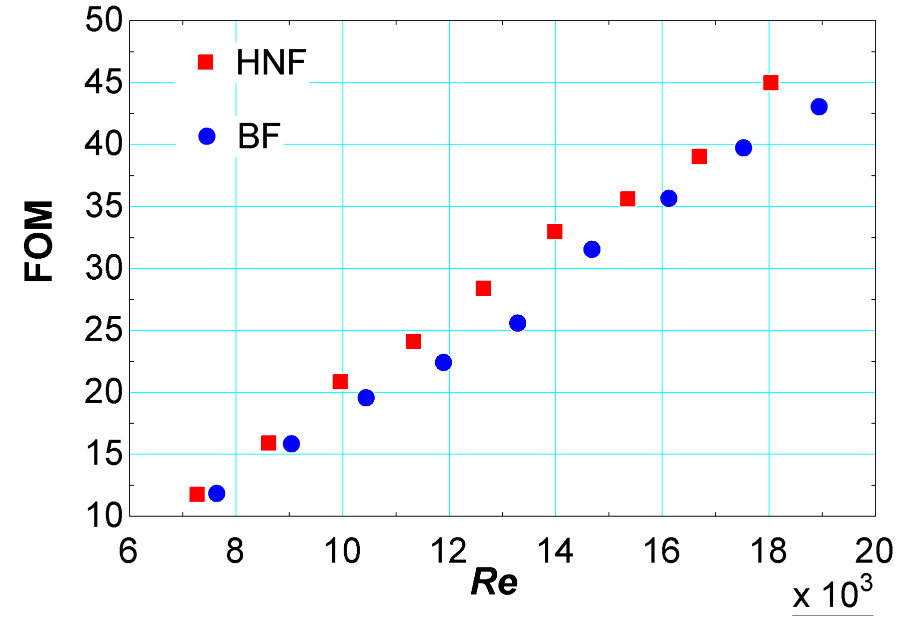

Figure 8. Figure of merit (FOM) versus Reynolds number for hybrid nano-oil 1% (V/V) of Al_2O_3-CuO-TVP1 and pure TVP1 oil.

3.5. Experimental Nusselt number comparison with Generalized Nusselt Number correlation

A thorough comparison between the experimentally determined Nusselt number and the predictions obtained using the generalized Nusselt number correlation (see eq. 6), has been conducted for the hybrid nano-oil under turbulent flow conditions. Figure 9 depicts the results of this comparison, demonstrating that the generalized Nusselt number correlation provides a reasonably good prediction of the experimentally obtained values, well within the proposed margin of ±15%, across the selected Reynolds number range. This in turn, indicates that the generalized Nusselt number correlation is indeed suitable for estimating the convective heat transfer coefficient for turbulent flow of hybrid nano-oil, which will serve as valuable input for the system-lelvel tool to assess the heat transfer with hybrid nano-oil. Therefore, the findings and the reported data will serve as a vehicle for researchers and engineers working on applications involving the turbulent flow of hybrid nano-oil for system design and analyses.

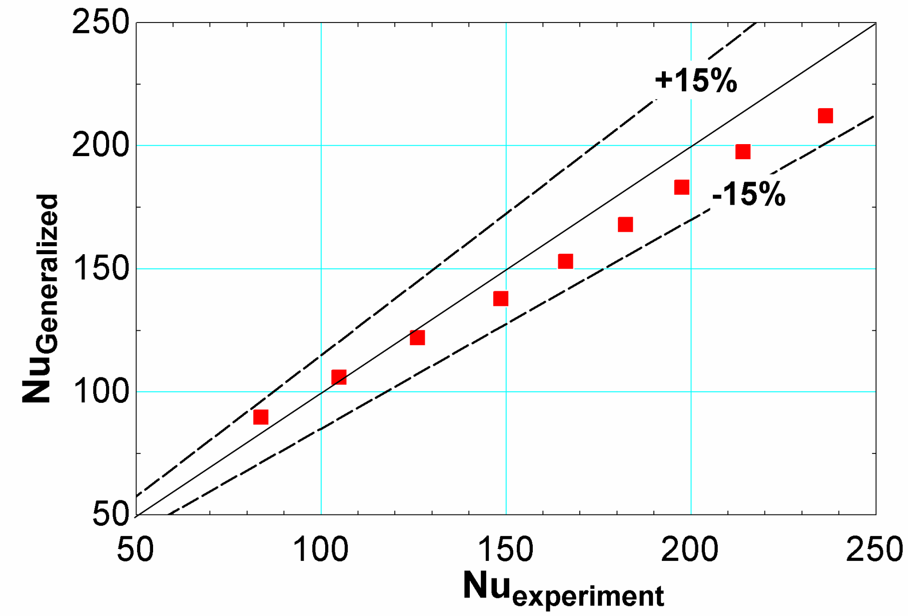

Figure 9. Comparison between experiment-based and generalized Nusselt number for hybrid nano-oil 1% (V/V) of Al_2O_3-CuO-TVP1.

3. Conclusions

This paper reports heat transfer experiments for turbulent flow of pure TVP1 and 1% (V/V) Al_2O_3-CuO-TVP1 hybrid nano-oil. The considered volume flow rates ranging from 10 to 26 LPM lead to Reynolds number in the range 7000 - 19000. The experimental setup involved a specially designed long, straight copper tube subjected to uniform heat flux conditions, simulating a parabolic trough absorber tube with secondary reflectors. The key findings and conclusions from these experiments are as follows:

- The hybrid nano-oil remained stable for up to 2 days, ensuring data reliability.
- Hybrid nano-oil exhibited a 15% improvement in surface area-averaged Nusselt number compared to TVP1, making it more efficient.
- However, hybrid nano-oil caused a 12% higher pressure drop, requiring more pumping power.
- The figure of merit (FoM = Nu/CP) for hybrid nano-oil was 5-6% higher than TVP1, indicating a favorable heat transfer-to-pressure drop ratio.
- It's recommended to use Al_2O_3-CuO-TVP1 hybrid nano-oil in parabolic trough absorbers for enhanced heat transfer and potentially reduced absorber length.
- The generalized Nusselt number correlation accurately predicted experimental values within ±15%, making it useful for analyzing heat transfer in the heated long tube.

Incorporating this correlation into system-level tools can enhance predictive capabilities for applications like the PTC absorber.

4. References

Gimeno-Furio et al., 2017. Stabilization and characterization of a nanofluid based on a eutectic mixture of diphenyl and diphenyl oxide and carbon nanoparticles under high temperature conditions. International Journal of Heat and Mass Transfer. 113, 908–913.

Klein, S. A., 2017. Engineering Equation Solver Professional Verison V10.215. F-chart Software Madison WI.

Krishna et al., 2018. State-of-the-art heat transfer fluids for parabolic trough collector. International Journal of Heat and Mass Transfer. 152, 119541.

Kumar, V., and Sarkar, J., 2019. Numerical and experimental investigations on heat transfer and pressure drop characteristics of Al2O3 -TiO2 hybrid nanofluid in minichannel heat sink with different mixture ratio. Powder Technology. 345, 717–727.

McClintock, F., and Kline, S., 1953. Describing uncertainties in single-sample experiments. Mech. Eng, 75. 3–8.

Mwesigye, A., and Meyer, J. P., 2017. Optimal thermal and thermodynamic performance of a solar parabolic trough receiver with different nanofluids and at different concentration ratios. Applied Energy. 193, 393–413.

Pak, B. C., and Cho, Y. I., 2013. Hydrodynamic and Heat Transfer Study of Dispersed Fluids with Submicron Metallic Oxide. Exp. Heat Transf. A J., Therm. Energy Transp., Storage, Convers. 11, 37–41.

Pranesh et al., 2019. A 50 year review of basic and applied research in compound parabolic concentrating solar thermal collector for domestic and industrial applications. Solar Energy. 187, 293-340.

Singh et al., 2005. Stability of dispersions of colloidal alumina particles in aqueous suspensions. Journal of Colloid Interface Sci. 291, 181–186.

Sousa, V. S., and Teixeira, M. R., 2013. Aggregation kinetics and surface charge of CuO nanoparticles: The influence of pH, ionic strength and humic acids. Environ. Chem., 10, 313–322, 2013.

Tang et al., 2021. A design method for optimizing the secondary reflector of a parabolic trough solar concentrator to achieve uniform heat flux distribution. Energy. 229, 120749.

Tiwari et al., 2021. A review on the application of hybrid nanofluids for parabolic trough collector: Recent progress and outlook. Journal of Cleaner Production. 292, 126031.

Upadhyay et al., 2021. A generalized Nusselt number correlation for nanofluids, and look-up diagrams to select a heat transfer fluid for medium temperature solar thermal applications. Applied Thermal Engineering. 190, 116469.

Upadhyay et al., 2022. Generalized Nusselt Number Correlation for Binary Hybrid Nano-Oils as Heat Transfer Fluid in Solar Thermal Systems. Journal of Heat and Mass Transfer ASME. 144, 1–10.

Vignarooban et al., 2015. Heat transfer fluids for concentrating solar power systems – A review. Applied Energy. 146, 383-396.

Xuan, Y., and Roetzel, W., 2000. Conceptions for heat transfer correlation of nanofluids. International Journal of Heat and Mass Transfer. 43, 3701–3707.